that Cp_2MoS_4 is not converted to Cp_2MoCl_2 upon low-energy irradiation in $CHCl_3$. Hence, the source of the Cp_2MoCl_2 in this experiment is not Cp_2MoS_4.) Two points argue against the top (heterolytic) route. First, according to this pathway Cp_2Mo^{2+} is an intermediate; it should be possible to trap this species. Yet even with large excesses of Cl^- present, we were unable to observe the formation of Cp_2MoCl_2 when Cp_2MoS_2 was irradiated in $(CD_3)_2SO$ or CD_3CN solvent. Second, the steady-state concentration of photoproduced S_2^{2-} will be quite low and consequently it seems unlikely that large amounts of S_2 will form via the (bimolecular) disproportionation process. This factor will tend to limit the amount of Cp_2MoS_4 formed.

It remains to discuss why *homolytic* extrusion of S_2 occurs when the Cp_2MoS_2 complex is irradiated. By analogy with the d-d band photochemistry of classical coordination complexes, one would expect the S_2 group to be extruded as S_2^{2-} when the complex is irradiated in the $14a_1 \rightarrow 9b_1$ d-d band (490 nm).[21] The covalency of the Mo-S bond (Figure 3d) may be responsible for the different behavior of the Cp_2MoS_2 complex.[22] Of course, irradiation at higher energy in the $6a_2 \rightarrow 9b_1$ S-Mo CT band (420 nm) is expected to lead to homolytic cleavage: the S_2^{2-} ligand is formally oxidized in the excited state and the Mo center is reduced.

Finally, as might be expected from the results of the calculation, Mo-Cp bond cleavage is not a primary photoprocess with the Cp_2MoS_2 complex. We were unable to observe the nitrosodurene-Cp spin-trapped radical under any of the photolysis conditions described in this paper.

In summary, we can now answer the two questions concerning S $\rightarrow$ MCT posed in the introduction to this paper. First, as with the Cp_2TiS_5 complex, S $\rightarrow$ MCT excitation in the Cp_2MoS_2 complex leads to homolytic M-S bond cleavage. Second, this behavior is not unique to S $\rightarrow$ MCT because d-d excitation of the Cp_2MoS_2 complex also leads to homolytic cleavage and the formation of S_2.

Acknowledgment is made to the Procter and Gamble Co. for the support of this research through a University Exploratory Research Grant. American Cyanamid is acknowledged for a fellowship to A.E.B.

Registry No. Cp_2MoS_2, 69228-83-7; Cp_2MoS_4, 54955-47-4.

Supplementary Material Available: The exact coordinates for the complex (including outer-sphere coordinates) and molecular orbital energies compositions (4 pages). Ordering information is given on any current masthead page.

(21) Zinato, E. In "Concepts of Inorganic Photochemistry"; Adamson, A., Fleischauer, P., Eds.; Wiley-Interscience: New York, 1975; Chapter 4.

(22) An alternative explanation is suggested by Balzani. See: Balzani, V.; Ballardini, R.; Sabbatini, N.; Moggi, I. *Inorg. Chem.* **1968**, *7*, 1398-1404.

Distortions in Coordinated Cyclopentadienyl Rings: Crystal, Molecular, and Electronic Structural Analysis of (η^5-Pentamethylcyclopentadienyl)dicarbonylrhodium[1]

Dennis L. Lichtenberger,* Charles H. Blevins, II, and Richard B. Ortega

Department of Chemistry, University of Arizona, Tucson, Arizona 85721

Received February 21, 1984

The crystal and molecular structure of $Rh(\eta^5\text{-}C_5(CH_3)_5)(CO)_2$ has been determined from a single-crystal X-ray diffraction study. The entire molecule approximates bilateral symmetry with the molecular mirror plane normal to the cyclopentadienyl ring and bisecting the $Rh(CO)_2$ fragment. The cyclopentadienyl C(ring)-C(ring) bond lengths consist of one short bond of 1.384 (8) Å adjacent to two long bonds of 1.445 (8) and 1.447 (7) Å, with the remaining two bonds having intermediate lengths of 1.412 (8) and 1.410 (7) Å. These bond distances are within one standard deviation of the distances found in the analogous cobalt complex. In addition, the cyclopentadienyl ring exhibits a slight symmetric distortion from planarity that significantly reflects the bonding between the ring and the metal. Molecular orbital calculations on an idealized geometry of $Rh(\eta^5\text{-}C_5H_5)(CO)_2$, in which the cyclopentadienyl ring is given D_{5h} symmetry, illustrate the electronic origin of the ring distortion. Calculated three-dimensional electron density maps show that the bonding of the ring to the metal is slightly dominated by a "dialkene" type interaction in which a single e_1^- orbital of the ring donates into an empty inplane metal d orbital of the d^8 $Rh(CO)_2^+$ portion of the molecule. The distortions of the ring are consistent with the character of this orbital. The title compound crystallizes in the monoclinic space group $P2_1/n$ with a = 7.765 (3) Å, b = 10.741 (3) Å, c = 15.267 (7) Å, β = 98.75 (3)°, and a calculated density of 1.551 g cm^{-3} for Z = 4. Full-matrix least-squares refinement with varying positional and anisotropic thermal parameters for the non-hydrogen atoms and idealized positional and isotropic thermal parameters for the hydrogen atoms converged at R_1 = 0.0339, R_2 = 0.0418, and GOF = 1.6818 (n = 136) for the 1610 independent reflections ($I \geq 3\sigma(I)$) collected with Mo Kα radiation over the 2θ range of 4° $\leq 2\theta \leq$ 50°.

Introduction

The cyclopentadienyl (Cp) ring has played a major role in the development of organometallic chemistry since the discovery of ferrocene in 1951.[2] A common feature in the investigation of organometallic chemistry has been the η^5 coordination of a cyclopentadienyl ring to a metal center. The Cp ring has turned out to be a rather versatile ligand and has been observed to coordinate to metal fragments in a number of different σ-[3,4] and "slipped" π-bonding

(1) Portions of this work have been presented at the 184th National Meeting of the American Chemical Society, Kansas City, MO, Sept 1982; American Chemical Society: Washington, DC, 1982; INOR 147.

(2) Kealy, T. J.; Pauson, P. L. *Nature (London)* **1951**, *168*, 1039.

0276-7333/84/2303-1614$01.50/0

orientations.[5-8] The various degrees and possibilities of π activation of the Cp ligand by metal fragments has been addressed and pursued in several molecular systems.[9]

Distortions *within* the metal-coordinated Cp rings can give a measure of the electronic symmetry and bonding capabilities of the metal center. The possibility of these distortions has attracted the attention of many research groups,[10-21] although definitive evidence for a distortion has generally been difficult to obtain. One source of this difficulty is often the librational motion of the ring, which increases the positional uncertainties of the individual carbon atoms in structural determinations. Recently, more precise determinations of the geometries have appeared, and differences in ring carbon–carbon bond distances on the order of 0.03 Å have been observed. For example, Fitzpatrick and Butler[20,21] have minimized the problem of ring librational motion in structural determinations of $CpM(CO)_3$ (M = Mn and Re) by carrying out the analysis at low temperatures. We have previously studied a large number of d^6 $CpML_3$ complexes by valence photoelectron spectroscopy[22-31] and have shown that the characteristic splitting of the ionizations primarily derived from the Cp ring e_1'' level is probable evidence for a distortion of the coordinated ring from fivefold symmetry in the gas phase,[29] consistent with the results of Fitzpatrick and Butler.[20,21] Anchoring the Cp ring with pentasubstitution also serves to decrease the positional uncertainties of the ring carbon atoms. Raymond et al.[18] have used this approach successfully in examining the Jahn–Teller distortion of decamethylmanganocene, and Byers and Dahl[19] have illustrated the utility of this approach in identifying the Cp ring distortion in $Cp^*Co(CO)_2$, where $Cp^* = \eta^5$-$C_5(CH_3)_5$.

This latter complex was of special interest to us because of our recent investigation of the ionizations of several d^8 complexes of the general form $CpML_2$.[32,33] The ionizations predominantly associated with the Cp e_1'' are apparently particularly sensitive to the electronic distribution at the metal center and to the geometrical distortion of the five-membered ring. We have observed large changes in these ionizations between d^6 and d^8 metal–Cp complexes, and, interestingly, between $CpCo(CO)_2$ and $CpRh(CO)_2$.[33] These ionization differences are consistent with differing degrees of Cp ring distortion and/or differing excited-state effects for the positive ion. A careful structural comparison of $Cp^*Rh(CO)_2$ with $Cp^*Co(CO)_2$ is then essential for understanding the differences between these analogues.

Table I. Crystallographic Data at 24 °C[a]

formula	$C_{12}H_{15}O_2Rh$
mol wt, g mol^{-1}	294.18
space group	$P2_1/n$ (No. 14; cell choice 2)
cell dimensions[b]	
a, Å	7.765 (3)
b, Å	10.741 (3)
c, Å	15.267 (7)
β, deg	98.75 (3)
V, Å^3	1258.5 (8)
Z	4
d_{calcd} g cm^{-3}	1.551
cryst shape	rectangular parallelepiped
cryst dimens, mm	0.1 × 0.3 × 0.3
radiation, Å	(Mo Kα) 0.710 73
monochromator	graphite crystal
supplied power	50 kV, 20 mA
data collection method	θ-2θ scan
scan speed, deg min^{-1}	variable (5.86-29.3), determined as function of peak intensity
scan range (2θ), deg	$K\alpha_1$ −1.0 to $K\alpha_2$ +1.0
ratio of total background time to peak scan time	0.5
std reflctns	(1,3,1), (1,4,−1), (2,3,−3) after every 97 readings
std dev of stds	2.1%
2θ limit, deg	$4 < 2\theta < 50$
no. of unique data	2458
no. of data used in the calculation	1610, $I \geq 3\sigma(I)$
abs coeff (μ), cm^{-1}	13.00 (Mo Kα)

[a] The standard deviation of the least significant figure is given in the parentheses in this table. [b] Cell dimensions were obtained from a least-squares refinement of setting angles of 24 reflections in the 2θ range from 4° to 50°.

(3) For instance: (a) Bennett, M. J.; Cotton, F. A.; Davison, A.; Faller, J. W.; Lippard, S. J.; Morehouse, S. M. *J. Am. Chem. Soc.* **1966**, *88*, 4371. (b) Forder, R. A.; Prout, K. *Acta Crystallogr., Sect. B* **1974**, *B30*, 491. (c) Calderon, J. L.; Cotton, F. A.; Legzdins, P. *J. Am. Chem. Soc.* **1969**, *91*, 2528. (d) Calderon, J. L.; Cotton, F. A.; DeBoer, B. G.; Takats, J. *J. Am. Chem. Soc.* **1970**, *92*, 3801. (e) Birkhahn, M.; Krommes, P.; Massa, W.; Lorberth, J. *J. Organomet. Chem.* **1981**, *208*, 161.

(4) (a) Atwood, J. L.; Rogers, R. D.; Hunter, W. E.; Bernal, I.; Brunner, H.; Lukas, R.; Schwarz, W. *J. Chem. Soc., Chem. Commun.* **1978**, 451. (b) Ducruix, A.; Felkin, H.; Pascard, C.; Turner, G. K. *J. Chem. Soc., Dalton Trans.* **1975**, 615. (c) Ducruix, A.; Pascard, C. *Acta Crystallogr., Sect. B* **1977**, *B33*, 3688.

(5) Wheatley, P. J. *Perspect. Struct. Chem.* **1967**, *1*, 1 and references therein.

(6) (a) Baker, E. C.; Raymond, K. N.; Marks, T. J.; Wachter, W. A. *J. Am. Chem. Soc.* **1974**, *96*, 7586. (b) Daroda, R. J.; Wilkinson, G.; Hursthouse, M. B.; Malik, K. M. A.; Thornton-Pett, M. *J. Chem. Soc., Dalton Trans.* **1980**, 2316. (c) Pasynskii, A. A.; Skripkin, Y. V.; Kalinnikov, V. T.; Porai-Koshits, M. A.; Antsyshkina, A. S.; Sadikov, G. G.; Ostrikova, V. N. *J. Organomet. Chem.* **1980**, *201*, 269.

(7) Johnson, J. W.; Treichel, P. M. *J. Am. Chem. Soc.* **1977**, *99*, 1427.

(8) (a) Huttner, G.; Brintzinger, H. H.; Bell, L. G.; Friedrich, P.; Bejenke, V.; Neugebauer, D. *J. Organomet. Chem.* **1978**, *145*, 329. (b) Kraus, H. J.; Werner, H.; Krüger, C. *Z. Naturforsch., B: Anorg. Chem., Org. Chem.* **1983**, *38B*, 733.

(9) For instance: (a) Dickson, R. S.; Michel, L. J. *Aust. J. Chem.* **1975**, *28*, 285. (b) Kowala, C.; Wailes, P. C.; Weigold, H.; Wunderlich, J. A. *J. Chem. Soc., Chem. Commun.* **1974**, 993. (c) Bell, L. G.; Brintzinger, H. H. *J. Organomet. Chem.* **1977**, *135*, 173. (d) Brintzinger, H. H.; Lohr, L. L., Jr.; Wong, K. L. T. *J. Am. Chem. Soc.* **1975**, *97*, 5146. (e) Cotton, F. A.; Rusholme, G. A. *J. Am. Chem. Soc.* **1972**, *94*, 402.

(10) Dunitz, J. D.; Orgel, L. E.; Rich, A. *Acta Crystallogr.* **1956**, *9*, 373.

(11) Dahl, L. F.; Wei, C. H. *Inorg. Chem.* **1963**, *2*, 713.

(12) MacDonald, A. C.; Trotter, J. *Acta Crystallogr.* **1964**, *17*, 872.

(13) Bennett, M. J.; Churchill, M. R.; Gerloch, M.; Mason, R. *Nature (London)* **1964**, *201*, 1318.

(14) Gerloch, M.; Mason, R. *J. Chem. Soc.* **1965**, 296.

(15) Churchill, M. R. *J. Chem. Soc., Chem. Commun.* **1965**, 86.

(16) Churchill, M. R. *Inorg. Chem.* **1965**, *4*, 1734.

(17) Coleman, J. M.; Dahl, L. F. *J. Am. Chem. Soc.* **1967**, *89*, 542.

(18) Freyberg, D. P.; Robbins, J. L.; Raymond, K. N.; Smart, J. C. *J. Am. Chem. Soc.* **1979**, *101*, 892.

(19) Byers, L. R.; Dahl, L. F. *Inorg. Chem.* **1980**, *19*, 277.

(20) Fitzpatrick, P. J.; Le Page, Y.; Butler, I. S. *Acta Crystallogr., Sect. B* **1981**, *B37*, 1052.

(21) Fitzpatrick, P. J.; Le Page, Y.; Sedman, J.; Butler, I. S. *Inorg. Chem.* **1981**, *20*, 2852.

(22) Whitesides, T. H.; Lichtenberger, D. L.; Budnik, R. A. *Inorg. Chem.* **1975**, *14*, 68.

(23) Petersen, J. L.; Lichtenberger, D. L.; Fenske, R. F.; Dahl, L. F. *J. Am. Chem. Soc.* **1975**, *97*, 6433.

(24) Lichtenberger, D. L.; Fenske, R. F. *Inorg. Chem.* **1976**, *15*, 2015.

(25) Lichtenberger, D. L.; Fenske, R. F. *J. Am. Chem. Soc.* **1976**, *98*, 50.

(26) Lichtenberger, D. L.; Sellman, D.; Fenske, R. F. *J. Organomet. Chem.* **1976**, *117*, 253.

(27) Campbell, A. C. M.S. Thesis, University of Arizona, Tucson, 1979.

(28) Hubbard, J. L.; Lichtenberger, D. L. *Inorg. Chem.* **1980**, *19*, 1388.

(29) Calabro, D. C.; Hubbard, J. L.; Blevins, C. H., II; Campbell, A. C.; Lichtenberger, D. L. *J. Am. Chem. Soc.* **1981**, *103*, 6839.

(30) Calabro, D. C.; Lichtenberger, D. L. *J. Am. Chem. Soc.* **1981**, *103*, 6846.

(31) Calabro, D. C.; Lichtenberger, D. L.; Herrmann, W. A. *J. Am. Chem. Soc.* **1981**, *103*, 6852.

(32) Calabro, D. C.; Lichtenberger, D. L. "Abstracts of Papers", 182nd National Meeting of the American Chemical Society, New York, Sept 1981; American Chemical Society: Washington, DC, 1981.

(33) Lichtenberger, D. L.; Calabro, D. C.; Kellogg, G. E. following paper in this issue.

In addition to presenting the structure of $Cp^*Rh(CO)_2$ and comparing it with that of $Cp^*Co(CO)_2$,[19] we discuss the electronic distribution in the Cp–metal fragment with the aid of molecular orbital (MO) calculations and two- and three-dimensional electron density maps. As will be shown, these $CpM(CO)_2$ systems offer an ideal operational test of ring distortions caused by electronic effects at the metal center.

Experimental Section

Preparation of Crystals. Pentamethylcyclopentadiene Cp^*H was prepared according to the method of Threlkel and Bercaw.[34] The route described by McCleverty and Wilkinson[35] was used for the preparation of $Rh_2Cl_2(CO)_4$. The synthesis of $Cp^*Rh(CO)_2$ was executed by using modifications of the procedure of Maitlis et al.[36] described as follows. Utilizing standard Schlenk techniques with a nitrogen atmosphere at 0 °C, 0.5 mL (3 mmol) of previously distilled Cp^*H, 1.0 mL (3 mmol) of a 2.4 M butyllithium/*n*-hexane solution, and 5 mL of freshly distilled hexane were added to a small round-bottom Schlenk vessel. This yellow solution was allowed to slowly warm to room temperature with constant stirring. After 12 h the solution had become milky white. To this solution of the lithium pentamethylcyclopentadienide was added 0.15 g (0.39 mmol) of $Rh_2Cl_2(CO)_4$ under dynamic N_2 flow. After 4 h of stirring at room temperature, the infrared (IR) spectrum of the hexane solution no longer displayed the characteristic carbonyl stretching frequencies of the starting $Rh_2Cl_2(CO)_4$ but rather exhibited two carbonyl peaks at 2012 and 1947 cm^{-1}, corresponding to the ν_{CO} of $Cp^*Rh(CO)_2$. The solvent was then removed in vacuo, and the residue was extracted with pentane and placed onto a Florisil column. A dark red-orange band was eluted from the column with methanol. The solvent was then removed in vacuo. Slow sublimation of this residue at 40 °C (10^{-1} torr) afforded several red-orange crystallographic quality crystals. The sublimed product's IR spectrum (KBr) exhibited two intense carbonyl stretching frequencies at 2000 and 1939 cm^{-1} corresponding to those observed by Maitlis et al.[36] at 2000 and 1950 cm^{-1}. The observed decomposition point of the product occurred at 79–80 °C.

Collection and Reduction of the X-ray Intensity Data. Due to the title compound's high voltaility, a crystal (0.3 × 0.3 × 0.1 mm) was completely encased in epoxy inside a glass capillary tube before being mounted onto a Syntex $P2_1$ autodiffractometer. The automatic centering, indexing, and least-squares routines were utilized to obtain the cell dimensions and standard deviations given in Table I, together with the other crystallographic data. An examination of the systematic absences in the collection data ($k = 2n + 1$ for $(0k0)$ and $h + l = 2n + 1$ for $(h0l)$) identified the space group as $P2_1/n$. A total of 2458 unique data were collected, of which 1610 reflections with $I \geq 3\sigma(I)$ were found and used for refinement. Due to unfortunate computer disk problems, no absorption corrections (on the basis of the calculated linear absorption coefficient, μ, of 13.00 cm^{-1} for Mo Kα radiation) could be applied to the initial solution. We have subsequently applied the absorption corrections by the method of Walker.[37] These corrections decreased the uncertainties in atomic positions by about 30% and improved the refinement to $R_1 = 3.1$, $R_2 = 3.6$, and GOF = 1.45. All positions remained the same within one standard deviation. We prefer to report here the more conservative uncertainties without the absorptions treatment. The results of the solution with empirical absorption corrections are included as supplementary material.

Solution and Refinement of the Structure. The neutral atomic scattering factors of Cromer and Waber[38] were used for all atoms. Anomalous dispersion corrections (Mo Kα radiation) were made for rhodium ($\Delta f' = -1.1$ and $\Delta f'' = 1.2$).

The structure was refined by using a full-matrix least-squares technique,[39] with refinement based on F_o with $\sum w(|F_o| - |F_c|)^2$ minimized. The weights were assigned as $w = 4F_o^2/[\sigma^2(F_o)^2 + (pF_o^2)^2]$, where p, the factor to prevent the overweighting of strong reflections, was set equal to 0.03. The unweighted and weighted discrepancy factors used were $R_1 = \sum||F_o| - |F_c||/\sum|F_o|$ and $R_2 = [\sum w(|F_o| - |F_c|)^2/w(F_o)^2]^{1/2}$. The "goodness of fit" is defined as GOF = $[\sum w(|F_o| - |F_c|)^2/(m - n)]^2$, where m is the number of reflections used in the refinement and n is the number of refined parameters.

A total of 1610 significant reflections ($I > 3\sigma(I)$) were used in the structural determination.[40] Each reflection was individually analyzed and intensity corrected by a profile analysis.[41] The position of the rhodium atom was resolved from the analysis of a Patterson synthesis.[42] The crystal and molecular structures were then determined from successive refinements and difference electron density maps that ultimately located all atoms. Least-squares refinement with varying positional and anisotropic thermal parameters for the non-hydrogen atoms and with idealized positional and isotropic thermal parameters for the hydrogen atoms converged to $R_1 = 0.0339$, $R_2 = 0.0318$, and GOF = 1.6818 ($n = 136$). The overdetermination ratio (m/n) was 11.84. The final electron density difference map revealed no peaks of electron density above 0.4 e Å^{-3}. The final non-hydrogen atomic parameters with their standard deviations are shown in Table II, and the final hydrogen atomic parameters are listed in Table III. Idealized hydrogen atomic parameters were obtained in the following manner. The hydrogen positional and isotropic thermal parameters were found and refined in order to obtain the relative orientation of the methyl groups to the ring. The hydrogens were then idealized in that orientation to 0.96-Å C–H bond lengths[43] and 109.50° H–C–H and C–C–H bond angles. The structure was then refined with these idealized hydrogens fixed. The isotropic thermal parameters of the hydrogen atoms were fixed at a value 50% greater than the refined isotropic thermal parameters of their corresponding methyl carbon atoms. Finally, it should be noted that the bond distances and angles discussed in this paper are largely insensitive to alternative reasonable methods of treating the hydrogen atoms, extinction corrections, absorption corrections, selection of significant reflections, and more sophisticated profile determination and analysis of the reflections. Tables of the observed and calculated structure factors are available as supplementary material.

Molecular Orbital Calculations. Approximate molecular orbital calculations were carried out by the parameter-free method of Fenske and Hall[25,44] on the prototype molecule $(\eta^5\text{-}C_5H_5)Rh(CO)_2$. Standard carbon, oxygen, and hydrogen (exponent of 1.2) functions were used. The rhodium(1+) functions were taken from Clementi and Roetti[45] and used directly. Gram–Schmidt orthogonal 5s and 5p functions with exponents of 2.0 for both were added to the rhodium basis. The calculation on the idealized C_s geometry used linear Rh–C–O groups with averaged bond distances. The (O)C–Rh–C(O) angle was idealized at 90°. The Cp ring was averaged to local D_{5h} symmetry with equidistant ring carbons (the average value of 1.420 Å) so that electronic factors are not determined by a distorted geometry. C–H distances were set to 1.09 Å, and all Rh–C(ring) distances were set to the averaged value of 2.258 Å.

The calculation of the molecule in its actual geometry involved averaging all of the *mirror-related* bond lengths and bond angles. The (O)C–Rh–C(O) angle was again idealized to 90°. Hydrogen atoms were used on the ring instead of methyl groups. The C–H

(34) Threlkel, R. S.; Bercaw, J. E. *J. Organomet. Chem.* **1977**, *136*, 1.
(35) McCleverty, J. A.; Wilkinson, G. *Inorg. Synth.* **1966**, *8*, 211.
(36) Kang, J. W.; Maitlis, P. M. *J. Organomet. Chem.* **1971**, *26*, 393.
(37) Walker, N.; Stuart, D. *Acta Crystallogr.* **1983**, *A39*, 159.
(38) Ibers, J. A.; Hamilton, W. C. "International Tables for X-ray Crystallography": Kynoch Press: Birmingham, England, 1974; Vol. IV.
(39) Ibers, J. A. "NUCLS8", adapted from "ORFLS", a Fortran Crystallographic Least-squares Program: Busing, W. R.; Martin, K. O.; Levy, H. A. Report ORNL-TM-305; Oak Ridge National Laboratory: Oak Ridge, TN, 1962.
(40) The 020 and 102 reflections were not used in the least-squares refinement due to detector overloading. Rescaling and inclusion of these two reflections' F_o values, as well as those for the $10\bar{1}$, 202, and 111 reflections, from a recollection of these five intensities made no difference in the results.
(41) Blessing, R. H.; Coppens, P.; Becker, P. *J. Appl. Crystallogr.* **1974**, *7*, 488. PROFILE detected the very intense reflections listed above that escaped software detection with the $P2_1$ tape routines.
(42) A local modification of Zalkin's FORDAP was used.
(43) Churchill, M. R. *Inorg. Chem.* **1973**, *12*, 1213.
(44) Hall, M. B.; Fenske, R. F. *Inorg. Chem.* **1972**, *11*, 768.
(45) Clementi, E.; Roetti, C. *Atom. Data Nucl. Data Tables* **1974**, *14*, 177.

Table II[a]

atom	x	y	z	B(11)	B(22)	B(33)	B(12)	B(13)	B(23)
Rh	0.13886 (5)	0.21575 (4)	0.115038 (28)	32.77 (19)	31.82 (19)	38.57 (20)	0.09 (17)	7.19 (13)	−3.33 (18)
O(1)	−0.1305 (7)	0.3809 (6)	0.0143 (4)	63.0 (27)	89 (4)	111 (4)	32.8 (27)	11.8 (27)	36 (3)
O(2)	−0.0963 (8)	0.1707 (6)	0.2487 (4)	87 (3)	111 (4)	77 (3)	20 (3)	49.2 (28)	26.8 (29)
C(11)	0.4319 (7)	0.2508 (5)	0.1356 (3)	32.0 (21)	40.0 (26)	39.5 (23)	−5.5 (19)	4.7 (19)	−4.3 (20)
C(12)	0.3669 (7)	0.2393 (5)	0.0445 (4)	32.6 (21)	34.1 (23)	42.1 (23)	−0.2 (18)	9.1 (19)	−0.8 (20)
C(13)	0.3045 (6)	0.1135 (5)	0.0271 (4)	27.8 (20)	35.3 (24)	43.2 (25)	0.0 (18)	7.9 (18)	−7.5 (21)
C(14)	0.3220 (7)	0.0519 (5)	0.1076 (4)	33.0 (22)	32.3 (24)	59 (3)	4.8 (19)	10.8 (21)	3.3 (23)
C(15)	0.3959 (7)	0.1376 (6)	0.1761 (4)	33.9 (23)	47.3 (28)	42.1 (25)	5.3 (22)	4.4 (19)	5.8 (24)
C(21)	0.5253 (8)	0.3624 (7)	0.1792 (4)	48 (3)	56 (4)	66 (4)	−12.2 (28)	7.7 (26)	−14 (3)
C(22)	0.3839 (8)	0.3367 (6)	−0.0256 (4)	53 (3)	50 (3)	53 (3)	−2.0 (26)	16.9 (25)	9.8 (27)
C(23)	0.2438 (8)	0.0587 (6)	−0.0634 (4)	47.0 (29)	62 (4)	54 (3)	−6.4 (27)	12.8 (24)	−21.8 (29)
C(24)	0.2817 (9)	−0.0848 (6)	0.1214 (6)	55 (3)	37.4 (28)	110 (5)	3.6 (27)	22 (3)	12 (3)
C(25)	0.4518 (9)	0.1051 (8)	0.2725 (4)	61 (4)	86 (5)	48 (3)	6 (3)	3.9 (27)	20 (3)
C(1)	−0.0287 (8)	0.3188 (6)	0.0516 (4)	40.4 (27)	51 (3)	60 (3)	8.6 (24)	12.7 (25)	6.6 (26)
C(2)	−0.0070 (8)	0.1875 (6)	0.1980 (4)	48.3 (29)	60 (4)	50 (3)	5.9 (25)	19.9 (25)	3.6 (26)

[a] Anisotropic thermal parameters are in the form $\exp[-0.25(h^2a^{*2}B(11) + k^2b^{*2}B(22) + l^2c^{*2}B(33) + 2hka^*b^*B(12) + 2hla^*c^*B(13) + 2klb^*c^*B(23))]$. Thermal parameters are ×10.

Table III

atom	x	y	z	B, Å²
H(11)	0.640	0.367	0.163	6.23
H(12)	0.534	0.355	0.242	6.23
H(13)	0.462	0.436	0.160	6.23
H(21)	0.500	0.335	−0.040	5.79
H(22)	0.361	0.418	−0.003	5.79
H(23)	0.302	0.319	−0.078	5.79
H(31)	0.211	0.125	−0.105	6.47
H(32)	0.145	0.006	−0.061	6.47
H(33)	0.337	0.011	−0.082	6.47
H(41)	0.182	−0.109	0.080	6.71
H(42)	0.258	−0.097	0.181	6.71
H(43)	0.380	−0.135	0.112	6.71
H(51)	0.448	0.178	0.308	7.41
H(52)	0.568	0.073	0.280	7.41
H(53)	0.375	0.043	0.290	7.41

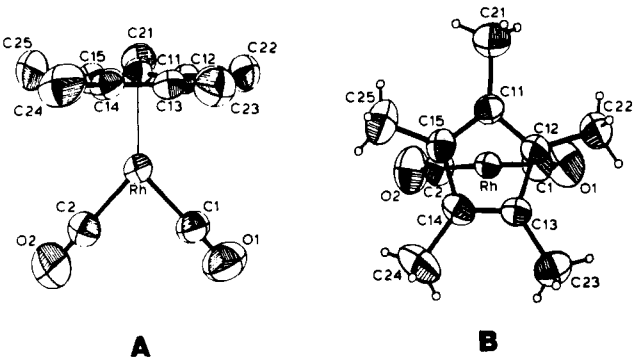

Figure 1. (A) The side-on view of the molecular configuration of $(\eta^5\text{-}C_5(CH_3)_5)Rh(CO)_2$ shown without the methyl hydrogen atoms. (B) The top view of the molecular configuration of $(\eta^5\text{-}C_5(CH_3)_5)Rh(CO)_2$. The thermal ellipsoids of these ORTEP diagrams are plotted at the 50% probability level.

bond lengths were all set to 1.09 Å, and their positions were placed along the appropriate averaged mirror-related C(ring)–C(methyl) vectors. Thus, the actual ring puckering and non-sp^2-like ring carbon bonding were incorporated into the molecular geometry for the calculation.

Two- and Three-Dimensional Electron Density Displays. The three-dimensional theoretical electron density difference map was generated by the program MO3D.[46] This electron density difference map (Figure 7A) was constructed by subtracting the calculated total electron density of Cp^- and a spherical rhodium atom from the calculated total electron density of $CpRh(CO)_2$. The generated maps were then rotated in three-dimensional space on an MMS-X graphics display system and plotted to achieve the final perspective shown in Figure 7A. The two-dimensional contour map was generated by the program MOPLOT.[47] This contour map (Figure 7B) describes the two-dimensional cross-section of the three-dimensional electron density difference map (Figure 7A), taken 0.5 Å below the plane of the ring carbon atoms. The difference contours in parts A and B of Figure 7 are the same. The outer contours represent the 0.75×10^{-2} difference level and every additional contour in Figure 7B represents a doubling of the previous contour.

The *experimental* two-dimensional electron density map shown in Figure 4 was obtained from a three-dimensional Fourier map[48] using the phases based upon the final least-squares refinement.[49] The plane shown is defined by atoms C(12), C(13), and C(15) (with C(14) being 0.004 Å out of this plane). The contours shown are in multiples of 0.1 e/Å^{-3}.

(46) MO3D is a modification (D. L. Lichtenberger) of MOPLOT[47] for three-dimensional electron density maps.

(47) Lichtenberger, D. L.; Fenske, R. F. *QCPE* **1975**, *10*, 284.

(48) "Structure Determination Package"; B.A. Frenz and Associates, Inc.: College Station, TX, and Enraf-Nonius, Delft, Holland.

(49) The 202 reflection's observed structure factor was set to its calculated value for the Fourier map. The F_o of the 10$\bar{1}$, 012, 111, and 020 reflections, unlike the 202, were successfully rescaled from subsequent measurements.[41]

Table IV. Interatomic Distances and Bond Angles for $Rh(\eta^5\text{-}C_5(CH_3)_5)(CO)_2$

A. Intermolecular Distances (Å)

Rh-C(1)	1.863 (6)	C(13)-C(14)	1.384 (8)	Rh-C(13)	2.278 (6)
Rh-C(2)	1.845 (7)	C(12)-C(13)	1.445 (8)	Rh-C(14)	2.276 (5)
av	1.856	C(14)-C(15)	1.447 (7)	av	2.277
C(1)-O(1)	1.121 (8)	av	1.446	C(15)-C(25)	1.511 (8)
C(2)-O(2)	1.129 (9)	Rh-C(15)	2.234 (5)	C(12)-C(22)	1.518 (9)
av	1.125	Rh-C(12)	2.222 (6)	av	1.515
C(11)-C(15)	1.412 (8)	av	2.228	C(11)-C(21)	1.503 (9)
C(11)-C(12)	1.410 (7)	Rh-C(11)	2.281 (5)	C(13)-C(23)	1.510 (8)
av	1.411			C(14)-C(24)	1.523 (9)
				av	1.517

B. Bond Angles (deg)

C(1)-Rh-C(2)	90.1 (3)	C(15)-C(14)-C(13)	108.3 (4)	C(25)-C(15)-C(14)	125.6 (4)
Rh-C(1)-O(1)	179.1 (5)	C(12)-C(13)-C(14)	107.3 (4)	C(22)-C(12)-C(13)	125.2 (4)
Rh-C(2)-O(2)	179.7 (5)	av	107.8	av	125.4
av	179.2	C(21)-C(11)-C(5)	127.4 (4)	C(15)-C(14)-C(24)	125.5 (4)
C(14)-C(15)-C(11)	108.3 (4)	C(21)-C(11)-C(12)	125.7 (4)	C(12)-C(13)-C(23)	125.6 (4)
C(11)-C(12)-C(13)	108.9 (4)	av	126.6	av	125.6
av	108.6	C(11)-C(15)-C(25)	125.4 (4)	C(24)-C(14)-C(13)	126.1 (4)
C(15)-C(14)-C(12)	106.9 (4)	C(11)-C(12)-C(22)	125.3 (4)	C(23)-C(13)-C(14)	127.0 (4)
		av	125.4	av	126.6

Results

Description of the Molecular Structure. The interatomic distances and bond angles for $Rh(\eta^5\text{-}C_5(CH_3)_5)(CO)_2$ are listed in Table IV. The molecular configuration (Figure 1A) consists of a rhodium atom bonded to one pentamethylcyclopentadienyl ligand and to two carbon monoxide ligands. The two Rh–C–O groups are nearly equivalent. They are essentially linear, and the (O)C–Rh–C(O) bond angle is 90°. The Rh–C–O distances are typical for $[CpRh(CO)_x]_y$ complexes.[50]

It is apparent from Figure 1B that the Cp* ligand is nearly symmetrically disposed relative to the planar $Rh(CO)_2$ fragment, even though these atoms are crystallographically distinct. This disposition maintains the approximate mirror plane that bisects the molecule by passing through the rhodium atom, one ring carbon atom (C(11)) and its attached methyl carbon atom (C(21)). As a consequence of the pseudomirror plane, C(12) and C(15) are approximately mirror-related as are C(13) and C(14) in addition to their corresponding methyl carbons and hydrogens. The deviation of the actual determined ring carbon positions from their mirror-related average positions is only 0.001 Å. Table IV and Figure 2 reveal that there is a significant distortion in the ring which also observes the mirror symmetry of the molecule. The cyclopentadienyl C(ring)–C(ring) bond lengths consist of one short bond of 1.384 (8) Å (C(13)–C(14)) adjacent to two statistically equivalent long bonds of 1.445 (8) and 1.447 (7) Å (C(12)–C(13) and C(14)–C(15)), with the remaining two statistically equivalent bonds having intermediate lengths of 1.412 (8) and 1.410 (7) Å (C(11)–C(12) and C(11)–C(15)). The differences between the long and short ring bonds are about 8σ, and the difference is significant at the 0.0001 probability level.[51]

Table V and Figure 1B both reveal two small symmetric distortions from planarity in the ten-carbon Cp* ring. The first observable distortion occurs within the five-membered carbon ring. Evidence for a slight ring puckering is given by the displacements from the plane defined by the five ring carbons. This puckering also appears to have mirror symmetry. Mirror-related ring carbons C(12) and C(15) deviate from this mean plane by 0.026 and 0.024 Å, respectively, toward the rhodium atom while carbons C(11), C(13), and C(14) deviate by 0.031, 0.011, and 0.008 Å, respectively, away from the rhodium. As a consequence, carbons C(12) and C(15) are 0.04–0.05 Å closer to the rhodium atom than the other three ring carbon atoms. The second distortion is the symmetric displacement of the methyl carbons above the ring and away from the rhodium atom. Mirror-related methyl carbons C(22) and C(25) deviate by 0.07 and 0.09 Å from the mean plane and methyl carbons C(23) and C(24) deviate by 0.13 and 0.11 Å, respectively. Carbon C(21) deviates the most, 0.16 Å, from this plane.

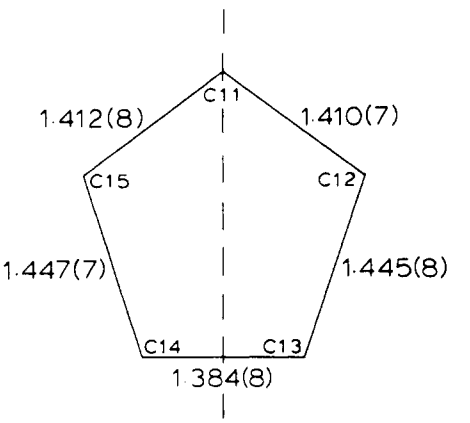

Figure 2. The crystallographically determined ring carbon internuclear bond distances in $(\eta^5\text{-}C_5(CH_3)_5)Rh(CO)_2$. The dashed line represents the plane of pseudomirror symmetry.

The deviation of each methyl carbon from the plane of the three nearest-neighbor ring carbons (as shown in the following figure)

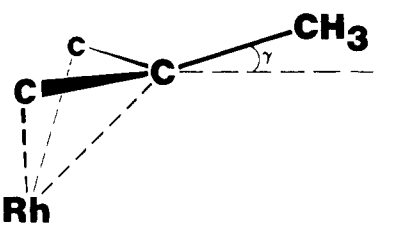

is more instructive for understanding the bonding of the Cp ring to the metal fragment and is a more accurate indication of the amount of ring carbon rehybridization. The planes that are defined by each methyl group's three nearest-neighbor ring carbon atoms will hereafter be re-

(50) (a) Mills, O. S.; Nice, J. P. *J. Organomet. Chem.* **1967**, *10*, 337. (b) Paulus, V. E. F. *Acta Crystallogr., Sect. B* **1969**, *B25*, 2206.

(51) Stout, G. H.; Jenson, L. H. "X-ray Structure Determination; A Practical Guide"; Macmillan: New York, 1968; pp 419–424.

Table V. Mean Planes and Interplanar Angles for $Rh(\eta^5\text{-}C_5(CH_3)_5)(CO)_2$[a-c]

A. Planes and Perpendicular Distances (Å) of Selected Atoms from These Planes

1. Plane Defined by Rh, C(1), C(2), O(1), and O(2)

$[-0.3199X - 0.7870Y - 0.5272Z - 2.9980 = 0]$

Rh	−0.0010	O(1)	−0.0010
C(1)	0.0015	O(2)	−0.0007
C(2)	0.0012	ORGN	0.0439

RMSD of fitted atoms from plane 0.0011 Å

2. Plane Defined by C(11), C(12), C(13), C(14), and C(15)

$[0.9413X - 0.3107Y - 0.1318Z + 1.7234 = 0]$

C(11)	0.0306	C(21)	0.1595
C(12)	−0.0256	C(22)	0.0665
C(13)	0.0109	C(23)	0.1273
C(14)	0.0077	C(24)	0.1118
C(15)	−0.0236	C(25)	0.0908

RMSD of fitted atoms from plane 0.0216 Å

3. Plane Defined by C(11), C(12), C(13), C(14), C(15), C(21), C(22), C(23), C(24), and C(25)

$[0.9408X - 0.3113Y - 0.1341Z - 1.7732 = 0]$

C(11)	−0.0272	C(21)	0.0992
C(12)	−0.0801	C(22)	0.0135
C(13)	−0.0418	C(23)	0.0782
C(14)	−0.0472	C(24)	0.0575
C(15)	−0.0817	C(25)	0.0296
ORGN	−0.0556		

RMSD of fitted atoms from plane 0.617 Å

4. Plane Defined by Rh, C(11), and C(21)

$[0.0447X + 0.4631Y - 0.8852Z - 0.4270 = 0]$

ORGN	0.0213

B. Angles (deg) between Normals to the Planes

plane 1-plane 2	89.262	plane 2-plane 4	89.054	plane 1-plane 4	84.941
plane 1-plane 3	89.155	plane 3-plane 4	89.147		
av	89.21	av	89.10		

[a] Equation to the least-squares is $LX + MY + NZ = D$. All atoms have been equally weighted. [b] RMSD = root-mean-square deviation. [c] ORGN = centroid of the cyclopentadienyl ring carbon atom positions.

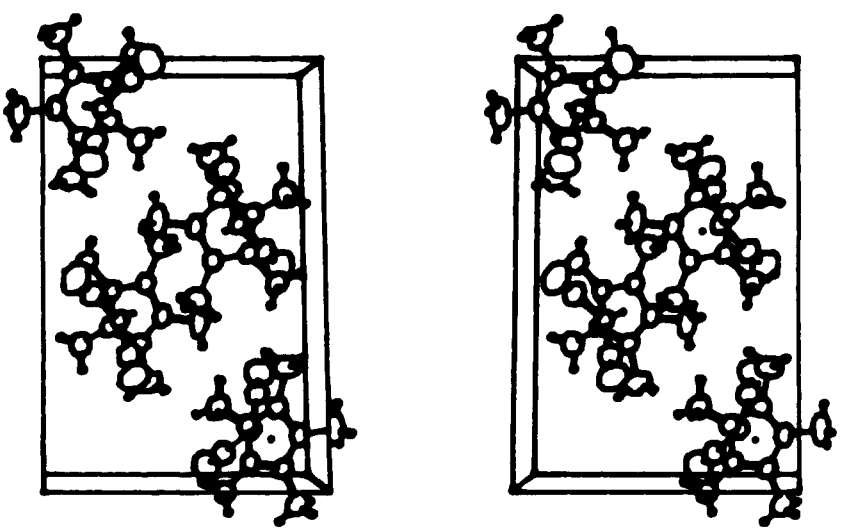

Figure 3. The stereoview of the unit cell packing diagram of $(\eta^5\text{-}C_5(CH_3)_5)Rh(CO)_2$.

ferred to as the methyl carbon's hybrid plane. Table VI shows the amount of deviation of each methyl carbon from their respective hybrid planes in terms of distance and also in terms of the angle γ. Again there is mirror symmetry in the deviations. Importantly, however, this analysis shows that the largest deviations are made by the mirror-related methyl carbons C(22) and C(25) with dispositions of 0.18 (6.8°) and 0.19 Å (7.2°), respectively. Mirror-related methyl carbons C(23) and C(24) both deviate from their hybrid planes by 0.08 Å (3.0°) and methyl carbon C(21) deviates the least (0.03 Å or 1.1°). We have also performed this same analysis on the Co analogue, and the results are included in Table VI and show a qualitatively similar rehybridization pattern.

Table V also reveals that the $Rh(CO)_2$ plane intersects the mean five-membered carbon ring at an angle of 89.26°. The resulting line of intersection on the Cp* ring passes within 0.044 Å of the ring centroid and virtually bisects the C(11)–C(15) and C(13)–C(14) bonds.

The unit cell projection shown in Figure 3 illustrates the relative orientations of the individual molecules. There is no indication of substantial steric overcrowding that would seriously effect the molecular geometry in the solid state. The closest intermolecular approaches are H···H and

Table VI. Distortion of Methyl Carbons from Their Nearest-Neighbor Carbon Ring Planes (Hybrid Planes)

	rhodium		cobalt[19]	
	l, Å	γ, deg	*l*, Å	γ, deg
C(21)	0.03	1.1	0.04	1.6
C(22)	0.18	6.8	0.13	5.1
C(25)	0.19	7.2	0.11	4.2
av	0.18	7.0	0.12	4.7
C(23)	0.08	3.0	0.07	2.7
C(24)	0.08	3.0	0.06	2.4
av	0.08	3.0	0.06	2.6

O···H in nature and are about 2.4 and about 2.7 Å, respectively.[52]

There is, however, a slight twisting (about 5°) of the (O)C–Rh–C(O) plane (mean plane 1 in Table V) from the otherwise orthogonality with respect to the pseudomirror plane (mean plane 4 in Table V) of the molecule. This is also noted in the cobalt complex. As shown in the following figure (taken from ref 52)

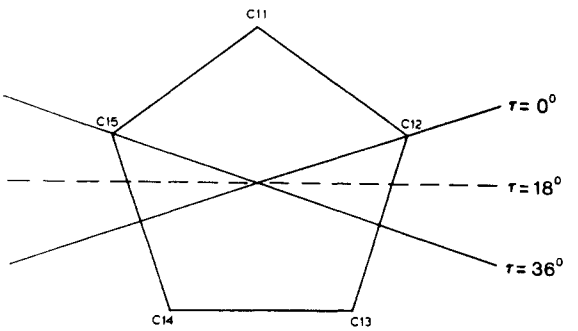

the two limiting forms of the relationship between the $M(CO)_2$ plane and the ring carbon atoms are the eclipsed and staggered arrangements. The eclipsed form may be defined as $\tau = 0$ and 36° where the solid lines projected on the ring correspond to the limits of the range of possible lines of intersection with the $M(CO)_2$ plane. The staggered configuration occurs when $\tau = 18°$ (dashed line). The observed angle, τ, in the Rh analogue is 12.9° and in the cobalt analogue is 13.9°. This may be attributable to intermolecular packing effects. The electron diffraction study of $CpCo(CO)_2$ in the gas phase, where intermolecular interactions of this sort are non-existent, yielded a τ value of 8 (7)°.[53] The uncertainty in the τ determination is so large that no conclusions can be drawn about the existence of a τ twist. The barrier to rotation of the Cp ring is low enough that even minimal intermolecular interactions in the crystal lattice may provoke such a twist. It can be seen in Figure 3 that the twist of the carbonyls with respect to the ring in a given molecule matches the misalignment of the pseudomirror plane of two molecules when they pack in the crystal. Although the eclipsed vs. staggered forms have been shown to switch upon the Cp → Cp* transformations in other systems,[54-57] no obvious pattern has emerged.

Figure 4 displays the *experimental* electron density in the σ-bonding framework of the Cp ring. The plane is

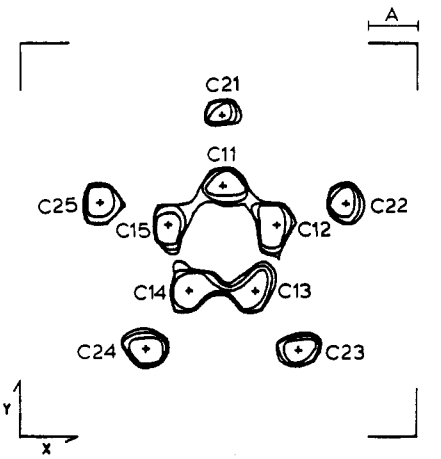

Figure 4. The experimental electron density map of the ten-carbon Cp ring showing the symmetric electronic distortion in the ring. The plane shown is defined by ring carbons C(11), C(13), and C(14). See text for discussion of this diagram.

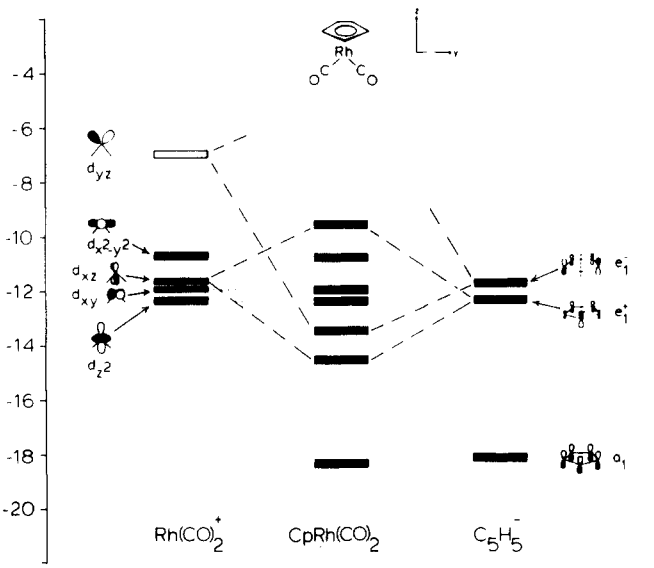

Figure 5. The molecular orbital correlation diagram of $(\eta^5\text{-}C_5(CH_3)_5)Rh(CO)_2$ including the fragment analysis of $Rh(CO)_2^+$ and Cp^- as obtained from the Fenske–Hall method. The actual molecular geometry (including the methyl groups) as determined by this study was used for this calculation.

defined by atoms C(11), C(13), and C(14) with C(15) very nearly in the plane. The figure illustrates the symmetric distortion away from fivefold symmetry of the electronic density in the region of the ring. There is a greater overlapping of C–C σ density in the short bond region between C(13) and C(14). There is an intermediate electron density value in the bond regions of C(11)–C(12) and C(11)–C(15), and the longest bonds C(12)–C(13) and C(14)–C(15) show the lowest electron density value in this region. It must be emphasized that the electronic distortion observed in this figure is not directly due to an electronic buildup/loss of bonding electron density in the different bonds. We do not feel that the experimental conditions and data are sufficient for definitive experimental bonding electron density studies of that sort. Rather, the observed electronic distortion in the ring in Figure 5 is primarily another way of representing the mirror-related differences in carbon–carbon bond lengths in the ring in this complex.

Discussion

Replacing a first-row transition metal in a complex with an isoelectronic second- or third-row metal frequently

(52) For this determination, the methyl C–H bonds were lengthened to the typical sp^3 internuclear 1.09 Å length.[43]

(53) Beagley, B.; Parrott, C. T.; Ulbrecht, V.; Young, G. G. *J. Mol. Struct.* **1979**, *52*, 47.

(54) Rausch, M. D.; Hart, M. P.; Atwood, J. L.; Zaworotko, M. J. *J. Organomet. Chem.* **1980**, *197*, 225.

(55) (a) Mills, O. S.; Nice, J. P. *J. Organomet. Chem.* **1967**, *9*, 339. (b) Bailey, N. A.; Radford, S. L.; Sanderson, J. A.; Tabatabaian, K.; White, C.; Worthington, J. M. *J. Organomet. Chem.* **1978**, *154*, 343.

(56) (a) Bryan, R. F.; Greene, P. T. *J. Chem. Soc. A* **1970**, 3064. (b) Mitschler, A.; Rees, B.; Lehmann, M. S. *J. Am. Chem. Soc.* **1978**, *100*, 3390. (c) Teller, R. G.; Williams, J. M. *Inorg. Chem.* **1980**, *19*, 2770.

(57) Adams, H.; Bailey, N. A.; White, C. *Inorg. Chem.* **1983**, *22*, 1155.

Table VII. Comparison of Ring Carbon Bond Distances and Angles and Selected Atoms' Deviations from the Mean Ring Plane for $M(\eta^5\text{-}C_5(CH_3)_5)(CO)_2$ where M = Co and Rh[a]

		Rh	Co
A. Corresponding Interatomic Ring Bond Distances (Å)			
C(11)-C(12)		1.410 (7)	1.407 (6)
C(11)-C(15)		1.412 (8)	1.414 (6)
	av	1.411	1.410
C(13)-C(14)		1.384 (8)	1.392 (6)
C(12)-C(13)		1.447 (7)	1.447 (6)
C(17)-C(15)		1.445 (8)	1.445 (6)
	av	1.446	1.446
B. Corresponding Ring Bond Angles (deg)			
C(14)-C(15)-C(11)		108.3 (4)	108.1 (4)
C(11)-C(12)-C(13)		108.9 (4)	108.9 (4)
	av	108.6	108.5
C(15)-C(11)-C(12)		106.9 (4)	107.4 (4)
C(15)-C(14)-C(13)		108.3 (4)	108.3 (3)
C(12)-C(13)-C(14)		107.3 (4)	107.1 (4)
	av	107.8	107.7
C. Planes and Perpendicular Distances (Å) of Selected Atoms from These Planes			
Plane Defined by C(11), C(12), C(13), C(14), and C(15)			
Rh: $0.9413X - 0.3107Y - 0.1318Z + 1.7234 = 0$			
Co: $0.9351X - 0.3159Y - 0.1608Z - 1.6327 = 0$			
metal		−1.909	−1.703
C(11)		0.031	0.021
C(12)		−0.026	−0.017
C(13)		0.011	0.007
C(14)		0.008	0.006
C(15)		−0.024	−0.016
C(25)		0.091	0.065
C(21)		0.060	0.131
C(22)		0.067	0.037
C(23)		0.127	0.092
C(24)		0.112	0.089

[a] Atom labels are those used for the Rh analogue as defined in this work.

changes the chemical properties of the complex. We have recently found from a photoelectron spectroscopic study of $Cp^*Co(CO)_2$ and $Cp^*Rh(CO)_2$ that the ionizations of these complexes differ significantly.[33] The differences are especially noteworthy in the ionizations of the predominantly ring e_1'' orbitals. These differences may be an indication of different degrees of electron localization and bonding in the ground states of these molecules, or they may be caused by differing excited-state effects in the positive ions of these complexes. The ground-state electron distribution and bonding can be reflected in the precise structural features of these complexes, and for this reason a careful comparison of the structures of $Cp^*Rh(CO)_2$ and $Cp^*Co(CO)_2$ was undertaken.

The results show that not only are $Cp^*Co(CO)_2$ and $Cp^*Rh(CO)_2$ isoelectronic but also they are isomorphous and isostructural. For instance, the C–O bond lengths are statistically equivalent to the analogous lengths in the Co complex as are the M–C–O bond angles (see Tables IV and VII and ref 19). The similarities in the C–O lengths, M–C–O and (O)C–M–C(O) angles, and coplanarity indicate that the total σ and π interactions of the metal with the carbonyl ligands is comparable in these two complexes. This is supported by the nearly identical infrared stretching frequencies and gas-phase core ionization energies.[33]

Of key importance in the structural comparison is that the ring distortions occurring in the Rh analogue are identical (within one standard deviation) with the distortions in the Co analogue as shown in Table VII. The lengthening of the two longest bonds in this system is

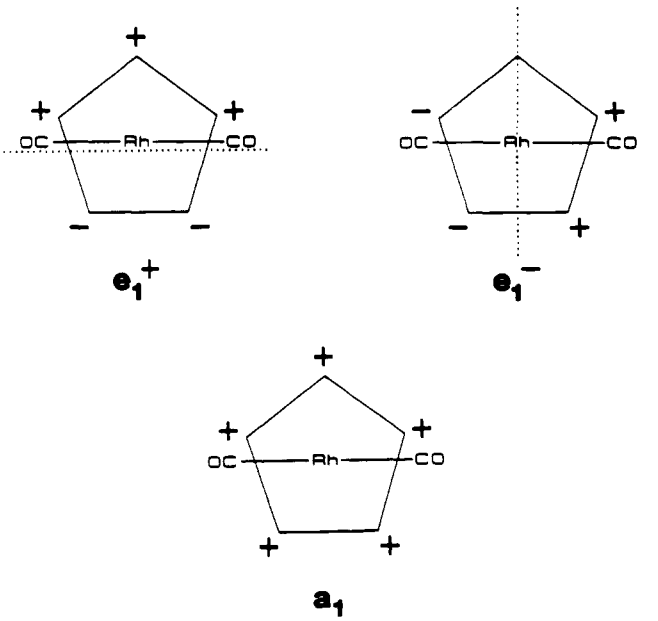

Figure 6. The symmetry orbitals of the cyclopentadienyl anion in relation to the (O)C–Rh–C(O) plane. The dotted line represents the nodes in the symmetry orbitals.

reminiscent of the effects of coordination in a monoolefin or dialkene-type complex where the localized π-bonding interactions in the carbon backbone decrease upon coordination so as to selectively lengthen the C=C bonds. Any alkyl or other groups bound to the C=C unit will also be bent away from the metal through rehybridization at the C=C centers. This bending is observed in the mirror-related five-carbon ring puckering and the symmetric disposition of the methyl carbons away from the metal atom. One manifestation of this puckering is that ring carbons C(12) and C(15) are significantly closer to the metal atom than the other three ring carbons (see Table IV). One additional common feature in the cobalt and rhodium analogues is that one hydrogen on each methyl carbon orients itself exo with respect to the metal, as also observed in other Cp*-metal species.[18,56c,58] In this Cp ring system the observed distortion appears to be from dialkene-like *bonding* to create a ring with an allyl–ene-type *structure*.

The primary features of the bonding and structure in complexes of this type have been discussed by Dahl[19] and follow simply from qualitative symmetry and electron occupation considerations. The molecular orbital correlation diagram of $(\eta^5\text{-}C_5H_5)Rh(CO)_2$ obtained with a Fenske–Hall calculation incorporating this crystal geometry is shown in Figure 5. The coordinate system for this discussion places the metal at the origin with the z axis projected toward the center of the Cp ring and the carbonyls placed in the d_{yz} plane. The fragment analysis of $Rh(CO)_2^+$ shows that the d_{yz} orbital (σ with respect to the carbonyls) is the only empty metal d orbital in this d^8 metal species. This region of low electron density is hybridized toward the Cp ring and is of the correct symmetry to accept electron density from the ring e_1^- fragment orbital (using Dahl's notation[19] for the fragment orbitals as shown in Figure 6). On the other hand the filled d_{xz} orbital is of the correct symmetry to mix with the ring e_1^+ fragment orbital that then stabilizes the resultant predominantly ring molecular orbital and destabilizes the predominantly metal d_{xz} orbital.

(58) Fernholt, L.; Haaland, A.; Seip, R.; Robbins, J. L.; Smart, J. C. *J. Organomet. Chem.* **1980**, *194*, 351.

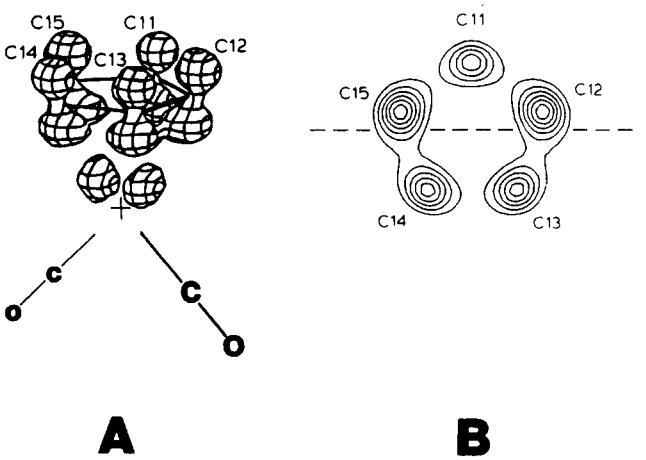

Figure 7. (A) The calculated three-dimensional electron density difference map of Cp^- and idealized $CpRh(CO)_2$. The difference map of idealized $CpRh(CO)_2$ and a Rh(0) atom is also shown. For simplicity, only the top two lobes of this "d_{yz}-like" orbital are shown. The right carbonyl is pointed out slightly toward the viewer. (B) The calculated electron density difference map of Cp^- and idealized $CpRh(CO)_2$ shown in two-dimensional space as sliced at 0.50 Å below the idealized Cp ring. The outer contour of this figure is identical with that in A (see text).

Our purpose is to illustrate the asymmetry in electron distribution with theoretically derived three-dimensional electron density maps and relate this to the structural geometry. As a first step in examining the asymmetry of the electron distribution, a model calculation was performed on $(\eta^5\text{-}C_5H_5)Rh(CO)_2$ with an idealized C_s geometry, a planar cyclopentadienyl ring, and all carbon–carbon bonds equidistant. The local fivefold symmetry of the ring ensures that any calculated asymmetry of the charge distribution is present before distortion is allowed. Figure 7A illustrates the primary changes in electron density that occur as a direct result of coordination of Cp^- to $M(CO)_2^+$. Electron density is lost from the ring primarily through ring carbon p-type orbitals, and electron density is gained by the metal primarily via a d_{yz}-type orbital. Also evident is that electron density is not donated symmetrically from the five carbon p orbitals. This may be clearly seen from the two-dimensional section taken at 0.5 Å below the Cp ring as shown in Figure 7B. The greatest amount of ring π density is donated from between ring carbons C(12)–C(13) and C(14)–C(15). This difference of density distribution relates directly to a greater donation from the ring e_1^- fragment orbital than from the e_1^+. This density distribution and bonding accounts for the distortion in bond lengths and the puckering of the ring. Because a greater proportion of density is removed from the e_1^- orbital, the bonding influence of this orbital on C(12)–C(13) and C(14)–C(15) will be diminished. These are the longest bonds evidenced by the structural determination. In addition, the antibonding influence of the e_1^- orbital on C(13)–C(14) will also be diminished. This is the shortest bond in the ring. Finally, e_1^- is localized primarily on C(12) and C(15), and the most stable geometry will favor placing these two carbons closer to the metal center than the others. The observed puckering of the Cp ring accomplishes this distortion.

Figure 7A also shows that the p orbitals from which electron density is lost are tilted slightly toward the metal center, as would be expected for maximum orbital overlap. This tilting requires a slight rehybridization of the ring carbon centers, and the effect of this may be seen in the symmetric disposition of the methyl carbons away from the rhodium atom (see Table VI). The same occurs in the cobalt analogue,[19] but to a lesser extent. The same rehybridization of the α-substituents to coordinated olefin carbons has previously been observed[59] and is understood in electronic terms.[30,60]

The results of this structural comparison of $Cp^*Rh(CO)_2$ with $Cp^*Co(CO)_2$ show that the ground states of both complexes are very similar. The cyclopentadienyl rings of both complexes have carbon–carbon bond distances that are distorted from fivefold symmetry to very nearly the same extent. The theoretical two- and three-dimensional electron density difference maps illustrate the preferential π donation of the filled e_1^- symmetry orbital into the empty d_{yz} orbital of the metal fragment (vs. the filled ring e_1^+ interaction with the filled d_{xz} orbital). It is this dialkene-like bonding that contributes to the observed allyl–ene-type Cp ring structures of these complexes.

Acknowledgment. We gratefully acknowledge the Department of Energy (Contract DE-AC02,80ER10746) and the University of Arizona for partial support of this research. We also wish to thank Dr. J. H. Enemark and Dr. W. N. Setzer for assistance with the structural data analysis and solution and Dr. P. Weber and Dr. F. R. Salemme for use of their MMS-X graphics display, as well as many helpful discussions. D.L.L. is an Alfred P. Sloan Fellow, and C.H.B. is a C.S. Marvel Fellow.

Registry No. $Cp^*Rh(CO)_2$, 32627-01-3.

Supplementary Material Available: Listings of observed and calculated structure amplitudes for the solution reported in this paper and listings of the results of the solution with empirical absorption corrections, including anisotropic thermal parameters, positional parameters, and selected bond distances and angles and observed and calculated structure amplitudes (22 pages). Ordering information in given on any current masthead page.

(59) (a) Guggenberger, L. J.; Cramer, R. *J. Am. Chem. Soc.* **1972**, *94*, 3779. (b) Aleksandrov, G. G.; Struchkov, Y. T.; Khandkarova, V. S.; Gubin, S. P. *J. Organomet. Chem.* **1970**, *25*, 243.
(60) Canadell, E.; Eisenstein, O.; Rubio, J. *Organometallics* **1984**, *3*, 759.